Neuro-Oncology
21(12), 1578–1586, 2019 | doi:10.1093/neuonc/noz141 | Advance Access date 17 October 2019

MRI radiomic features are associated with survival in melanoma brain metastases treated with immune checkpoint inhibitors

Ankush Bhatia,* Maxwell Birger,* Harini Veeraraghavan, Hyemin Um, Florent Tixier, Anna Sophia McKenney, Marina Cugliari, Annalise Caviasco, Angelica Bialczak, Rachna Malani, Jessica Flynn, Zhigang Zhang, T. Jonathan Yang, Bianca D. Santomasso, Alexander N. Shoushtari,† and Robert J. Young†

Department of Neurology (A.B., R.M., B.D.S.), Department of Radiology (M.B., A.S.M., R.J.Y.), Department of Medical Physics (H.V., H.U., F.T.), Department of Medicine (M.C., A.C., A.B., A.N.S.), Department of Epidemiology and Biostatistics (J.F., Z.Z.), and Department of Radiation Oncology (T.J.Y.), Memorial Sloan Kettering Cancer Center, New York, New York

Corresponding Author: Ankush Bhatia, MD, Brain Tumor Service, Department of Neurology, Memorial Sloan Kettering Cancer Center, 1275 York Avenue, New York, New York 10065 USA (ankushbhatia1@gmail.com).

*Authors contributed equally as co-first authors.

†Authors contributed equally as co-senior authors.

Abstract

Background. Melanoma brain metastases historically portend a dismal prognosis, but recent advances in immune checkpoint inhibitors (ICIs) have been associated with durable responses in some patients. There are no validated imaging biomarkers associated with outcomes in patients with melanoma brain metastases receiving ICIs. We hypothesized that radiomic analysis of magnetic resonance images (MRIs) could identify higher-order features associated with survival.

Methods. Between 2010 and 2019, we retrospectively reviewed patients with melanoma brain metastases who received ICI. After volumes of interest were drawn, several texture and edge descriptors, including first-order, Haralick, Gabor, Sobel, and Laplacian of Gaussian (LoG) features were extracted. Progression was determined using Response Assessment in Neuro-Oncology Brain Metastases. Univariate Cox regression was performed for each radiomic feature with adjustment for multiple comparisons followed by Lasso regression and multivariate analysis.

Results. Eighty-eight patients with 196 total brain metastases were identified. Median age was 63.5 years (range, 19–91 y). Ninety percent of patients had Eastern Cooperative Oncology Group performance status of 0 or 1 and 35% had elevated lactate dehydrogenase. Sixty-three patients (72%) received ipilimumab, 11 patients (13%) received programmed cell death protein 1 blockade, and 14 patients (16%) received nivolumab plus ipilimumab. Multiple features were associated with increased overall survival (OS), and LoG edge features best explained the variation in outcome (hazard ratio: 0.68, $P = 0.001$). In multivariate analysis, a similar trend with LoG was seen, but no longer significant with OS. Findings were confirmed in an independent cohort.

Conclusion. Higher-order MRI radiomic features in patients with melanoma brain metastases receiving ICI were associated with a trend toward improved OS.

Key Points

1. MRI radiomics are a potential biomarker of intratumoral heterogeneity.
2. MRI radiomics are associated with survival in melanoma brain metastases treated with ICIs.

© The Author(s) 2019. Published by Oxford University Press on behalf of the Society for Neuro-Oncology. All rights reserved.
For permissions, please e-mail: journals.permissions@oup.com

Importance of the Study

Immune checkpoint inhibition has drastically changed the treatment and prognosis of patients with melanoma brain metastases. However, there remains a subset of patients who do not respond intracranially and require additional treatment with surgery and/or radiation, likely due to intratumoral heterogeneity. In this manuscript, we demonstrate that MRI radiomic features on baseline neuroimaging are associated with overall survival for patients with melanoma brain metastases. These data suggest that MRI radiomics can be used as a potential biomarker to predict intratumoral heterogeneity and risk of intracranial progression. Incorporation of MRI radiomic features into future clinical trials will help elucidate their utility in practice.

Brain metastases are a leading cause of both neurological disability and death in patients with systemic malignancies.[1] Patients with melanoma have the highest risk of developing brain metastases among all patients with solid tumors.[2–4]The incidence of melanoma brain metastases has been described as 40–60% at some point during the course of disease but may be as high as 70% at autopsy.[4–6] Brain metastasis research has been inadequate over the years due to the exclusion of patients from clinical trials, inaccurate assumptions about prognosis, unclear radiographic response criteria, and the poor understanding of drug penetration across the blood–brain barrier.[1,7] Fortunately, the discovery of immune checkpoint inhibitors (ICIs), including antibodies to cytotoxic T lymphocyte antigen 4 (CTLA-4; ipilimumab) and programmed cell death protein 1 (PD1) (pembrolizumab and nivolumab), has dramatically changed the prognosis and treatment of melanoma brain metastases and has been a promising area of research.[8–10] A recent study evaluating the overall survival (OS) of patients who presented with cutaneous melanoma brain metastases during 2010–2015 using the National Cancer Database demonstrated a significantly improved median OS of 12.4 months in patients with melanoma metastases both intracranially and extracranially, representing a shift from a historical OS of only 4 months.[11] However, while a subset of patients respond to treatment with ICI and go on to achieve long-term remission, there persists a subset of patients who do not respond and have poor survival as a direct result of intracranial progression, creating an increasingly difficult clinical challenge of determining which patients should receive immunotherapy, concurrent radiation, and/or surgical resection. Given the heterogeneity in response to ICIs and the variation in the management of these patients, there is an increasing need for biomarkers that can predict therapeutic response and outcomes.

Genomic heterogeneity within a single brain metastasis has been hypothesized to be the most likely explanation for variations in response to ICIs, radiation, or surgery. This was exemplified by a recent study in which the authors conducted multiregion sampling of melanoma metastases and demonstrated heterogeneous gene-expression patterns within single lesions.[12,13] However, another study demonstrated that spatially and temporally separated brain metastatic lesions are genetically homogeneous, while distal extracranial metastases are highly divergent and genetically heterogeneous.[14] The complex interplay of genes, proteins, and cellular microenvironments within each metastasis can dictate the aggressiveness of the cancer and each patient's response to treatment.

In response to the dilemma as to managing melanoma brain metastases as described above, in this study we extracted radiomic texture and edge features from standard-of-care magnetic resonance imaging (MRI) to produce a range of quantitative parameters (features) that characterize the spatial variation of gray levels throughout an image.[15,16] Radiomics have been applied in the context of several diseases to aid in diagnosis and assessment of response to treatment, characterize heterogeneity, and predict survival.[17–31] In this study, we hypothesized that texture analysis of contrast T1-weighted MRI will identify higher-order features of melanoma brain metastases that are correlated with progression-free survival (PFS) and OS.

Materials and Methods

Study Data

This retrospective study was granted a waiver of informed consent by the institutional review board and was performed in compliance with Health Insurance Portability and Accountability Act regulations. We identified 377 consecutive patients with metastatic melanoma and brain metastases who received ipilimumab with or without nivolumab, nivolumab, or pembrolizumab between 2010 and 2017. Inclusion criteria were (1) age greater ≥18 years, (2) biopsy-proven metastatic melanoma, and (3) MRI of the brain with contrast performed within 3 months of developing brain metastases and before receiving ICIs. Patients were excluded if (1) they received ICIs prior to the development of brain metastases, (2) they received radiotherapy to brain metastases prior to the baseline MRI, or (3) brain metastases did not meet criteria for measurable disease per criteria of the Response Assessment in Neuro-Oncology Brain Metastases (RANO-BM) (<0.5 cm).[32] Patients receiving planned concurrent stereotactic radiosurgery (SRS) or whole-brain radiotherapy (WBRT) with ICI were included. Clinical data were collected such as age, sex, Eastern Cooperative Oncology Group (ECOG) performance status, lactate dehydrogenase (LDH) levels, planned treatment with ICI or radiation, prior systemic therapy for extracranial disease, driver mutational status, and melanoma subtype (summarized in Table 1). An additional independent cohort was obtained with similar methodology as above spanning 2017–2019.

Table 1 Clinical characteristics

Clinical Characteristics	*N* (%)
Age, years, mean (range)	63.5 (19–91)
Sex	
Male	57 (65)
Female	31 (35)
ECOG	
0	49 (56)
1	30 (34)
2/3	9 (10)
LDH	
Elevated	31 (35)
Normal	37 (42)
Unknown	20 (23)
Checkpoint inhibitor	
CTLA-4	63 (72)
PD1	11 (13)
PD1+ CTLA-4	14 (16)
Concurrent radiation	69 (78)
SRS	40 (45)
WBRT	29 (33)
Prior systemic therapy	42 (48)
BRAF ± MEK inhibitor	32 (36)
Chemotherapy	10 (11)
Driver mutational status	
BRAF V600E	37 (42)
Ras	17 (19)
NF1	4 (5)
Other	3 (3)
WT	16 (18)
Unknown	11 (13)
Melanoma subtype	
Cutaneous	60 (68)
Unknown	20 (23)
Mucosal	4 (5)
Acral	4 (5)

Abbreviations: NF1, neurofibromatosis type 1; WT, wild type.

MRI Acquisition

MRI was performed on 3T (n = 34) and 1.5T (n = 54) systems (750w/450w, GE Healthcare). Conventional MRI was acquired including axial contrast-enhanced T1-weighted images at 5 mm (n = 113), 4 mm (n = 2), or 3 mm (n = 3).

Image Segmentation

A maximum of 5 metastatic lesions were selected in patients with multiple metastases per RANO-BM guidelines.[33] If a patient had more than 5 metastatic lesions, the largest 5 target lesions by volume were chosen. Metastasis segmentation was manually performed by a trained operator (with 1 year of experience) using ITK-SNAP version 3.4.0 (www.itksnap.org).[34] The volume of interest of each metastatic lesion was verified by an experienced neuroradiologist (with >20 years of experience). If a lesion had gross precontrast T1 hyperintensity, this area was not segmented and not included in the analysis.

Radiomic Feature Analysis

First-order texture features, Haralick texture features, as well as Gabor, Sobel, and Laplacian of Gaussian (LoG) edge features were extracted from each metastatic lesion using the publicly available software Computational Environment for Radiotherapy Research (CERR)[35]; a total of 21 features were extracted per lesion from contrast-enhanced T1-weighted images. Normalization of imaging was not done as to support easy replication of methodology and use only those texture features that are robust to variations in image acquisitions.

The histogram-based first-order texture features included the mean, standard deviation, skewness, and kurtosis of the signal intensity of the pixels enclosed in the region of interest. The Haralick texture features[16] extracted in this study included energy, entropy, contrast, homogeneity, and correlation. The Haralick texture features, known also as second-order texture features, were computed from gray level co-occurrence matrices (GLCM) that described the spatial relationship of two pixels at a given offset and thus offered more information than first-order texture features. Thirteen directional offsets and a distance of 1 between the voxels were used for the 3-dimensional GLCM. One co-occurrence matrix was produced by combining the contributions from all offsets and was used to calculate the 5 textures. Further details on these features and the methods used to extract them have been published previously.[30, 36]

Gabor features are edge features computed to capture edges at different spatial scales and orientations.[37] In Gabor texture feature extraction, a filter bank is used to derive multiple filtered images from the original image. Each filtered image contains a subset of frequencies and orientations. In this study, one filter was used (bandwidth 2, angle 0°) and then first-order features were calculated from the regions of interest, resulting in 4 Gabor texture features. In addition, Sobel and LoG edge features were computed to describe spatial discontinuities in image signal intensity. A default MATLAB kernel size of 3 × 3 was implemented for the aforementioned filters. In this study, 4 features were extracted from the Sobel- and LoG-filtered images, leading to a total of 12 edge detection features.

Outcomes

The primary outcomes were PFS and OS. OS was defined as the date of the start of the ICI to the date of the last follow-up or the date of death. PFS was defined as the date of the start of ICI to the date of an unplanned change in treatment—for example, progression of disease as determined based on RANO-BM guidelines, unplanned local therapy

such as surgery (with pathology confirmed as disease), or radiation with SRS or WBRT.

Statistical Analysis

To determine the radiomic features that are relevant for OS, a weighted average of each radiomic feature across each patient's metastasis was taken. These averages were weighted by metastasis volume, which was calculated during segmentation. In other words, metastases with larger volumes were assigned a larger importance in deriving the radiomic features for each patient. This computation was done to extract an overall summary heterogeneity measure across all the metastases. A univariate Cox regression was employed to assess each radiomic feature as well as several clinical factors. A subsequent false discovery rate (FDR) adjustment for multiple comparisons was applied to the radiomic features. Because several features achieved significance ($P < 0.001$) and were found to be highly internally correlative, Lasso regression was performed[38] to reduce the number of features and to select a small set of features that are most relevant to OS.[39]

To determine the radiomic features relevant for PFS, progression analysis was conducted using a univariate competing risks regression model with competing risk of death without progression of disease. A clustering effect at the patient level was assumed due to several patients having multiple lesions, and an FDR correction was applied to the radiomic features.

To determine the degree of variability or heterogeneity in radiomic signatures among patients with multiple

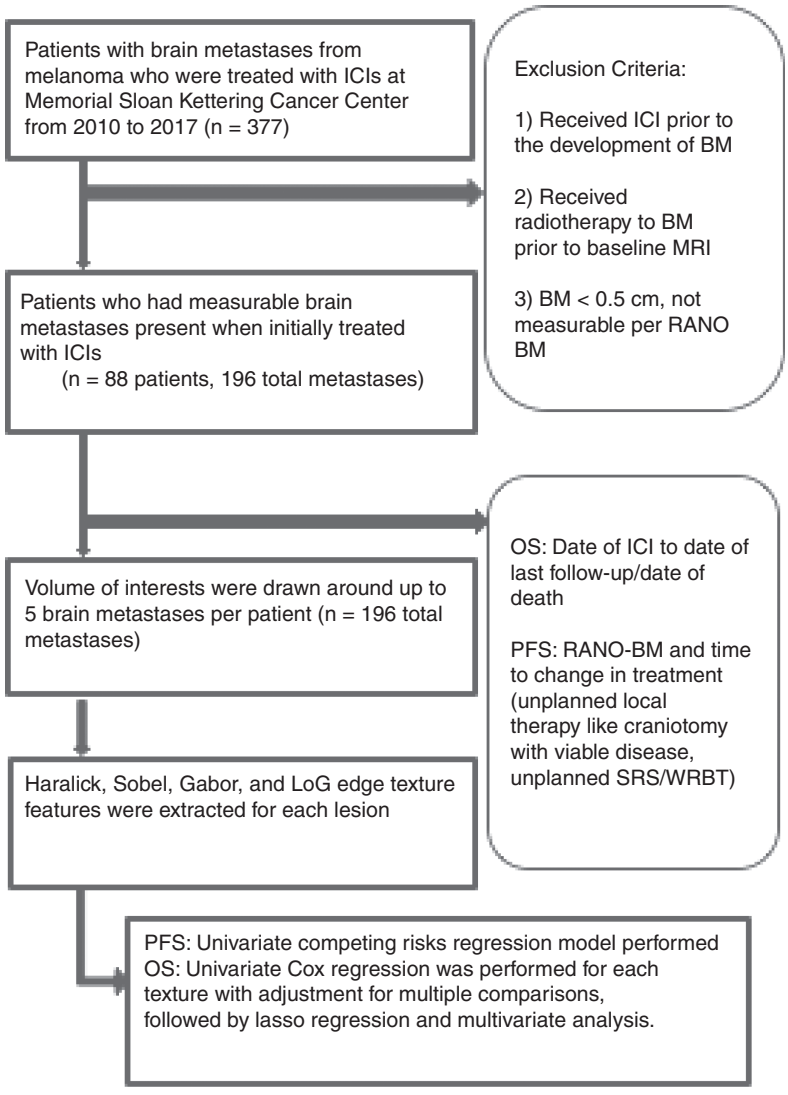

Fig. 1 CONSORT diagram.

brain metastases (n = 45), the range of mean LoG was calculated in each patient with multiple lesions and reported. Intrapatient variability was then compared with interpatient variability in the entire cohort.

Results

Clinical Characteristics

A total of 88 patients with 196 total metastases were included in the study (Fig. 1). Table 1 summarizes the clinical demographics of the study population. The median age in this retrospective study was 63.5 years (range, 19–91 y) and 65% of patients were male (57/88). Most patients had an ECOG performance status of 0 or 1 (90%) and 35% had elevated LDH. Sixty-three patients (72%) received ipilimumab, 11 patients (13%) received PD1 blockade in the form of monotherapy, and 14 patients (16%) received combination nivolumab plus ipilimumab. Most patients received planned concurrent radiation (78%). Forty-six patients (52%) were naïve to systemic therapy. Of those with prior systemic therapy, most received targeted BRAF ± MEK inhibition (32 patients, 36%). The most common driver mutation in our cohort was BRAF V600E, which was found in 37 patients (42%). Other relevant mutations seen were Ras in 17 patients (19%) and neurofibromatosis 1 in 4 patients (5%). The majority of patients had cutaneous melanoma (68%), but several patients were either unknown primary (23%) or mucosal (5%) or acral (5%).

MRI Radiomic Features

Table 2 summarizes the results of the univariate analysis to determine the impact of clinical variables on patient survival. Elevated LDH levels were found to be significantly associated with survival (P = 0.017). No other clinical variables were associated with survival, including age, ECOG performance status, elevated LDH, liver involvement, therapy type, radiation, or driver mutational status. Table 3 summarizes the results of the univariate analysis to determine the impact of radiomic features on patient OS. Multiple radiomic features were associated with increased OS. The mean LoG was the most relevant radiomic feature for explaining the variation in outcome (hazard ratio [HR]: 0.68, P = 0.001). Table 4 shows the results of multivariate analysis including mean LoG, LDH level, and ECOG performance status 0 versus ≥1. At multivariate analysis, a similar trend for higher mean LoG and better OS was seen, but it was no longer statistically significantly associated with OS when LDH and ECOG performance status were incorporated into the analysis. There were no significant differences found in PFS for any of the radiomic features following FDR correction or for any of the clinical factors.

Figure 2 demonstrates a representative image of 2 brain metastases with varying outcomes to checkpoint inhibition. These metastases appear similar on T1-weighted imaging, but clear differences could be detected in mean LoG post filtering as well as entropy.

Table 2 Univariate analysis of the impact of clinical variables on overall survival

	HR (95% CI)	*P*-value
Age	1.0 (0.99, 1.02)	0.823
ECOG		
0	1.00	0.255
1 + 2 + 3	1.33 (0.82, 2.16)	
Elevated LDH		
N	1.00	**0.017**
Y	1.96 (1.13, 3.4)	
Liver involvement		
N	1.00	0.173
Y	1.43 (0.85, 2.4)	
Checkpoint inhibitor		
PD1 + CTLA-4	1.00	0.232
CTLA-4	1.02 (0.5, 2.07)	
PD1	0.49 (0.17, 1.37)	
Concurrent radiation		
WBRT	1.00	0.23
SRS	0.72 (0.42, 1.23)	
Prior systemic therapy		
Chemotherapy	1.00	0.943
BRAF ± MEK inhibitor	1.03 (0.44, 2.32)	
Prior BRAF inhibitor		
No	1.00	0.17
Yes	1.63 (0.81, 3.29)	
Driver mutational status		
BRAF V600E	0.73 (0.38, 1.42)	0.36

Variability in Radiomic Signatures

To better understand the variability in radiomic signatures among different metastatic lesions within the same patient, the LoG variability ranges were reported in the 45 patients with multiple metastatic lesions (Supplementary Table 1) with the minimum and maximum ranges (0.0144, 1.8489). While there is no clear texture feature that measures heterogeneity, these tight ranges suggest more homogeneity of lesions within the same patient, compared with lesions between different patients. Supplementary Fig. 1 shows intrapatient variability of the feature; mean LoG is lower in 67% of the patients than the interpatient variability across the entire cohort.

Validation Cohort

To confirm the findings that mean LoG is an important radiomic feature, a new dataset (n = 17) was obtained at our institution. Using this independent dataset, the multivariate analysis findings were confirmed (Table 5). Namely, ECOG was significantly associated with OS (P = 0.01). Additionally, LDH was also associated with OS

Table 3 Univariate analysis of the impact of MRI radiomic features on overall survival

Feature Category	Feature Name	HR (95% CI)	*P*-value
Haralick	Entropy	0.33 (0.17, 0.64)	**0.001***
LoG	Mean	0.68 (0.54, 0.85)	**0.001***
LoG	Standard deviation	0.76 (0.65, 0.89)	**0.001***
Gabor	Mean	0.41 (0.24, 0.68)	**0.001***
Sobel	Mean	0.89 (0.83, 0.96)	**0.002***
Sobel	Standard deviation	0.86 (0.78, 0.95)	**0.004***
First order	Mean	0.93 (0.88, 0.98)	**0.005***
Gabor	Kurtosis	0.8 (0.68, 0.94)	**0.007***
Haralick	Contrast	0.92 (0.87, 0.99)	**0.016***
First order	Standard deviation	0.97 (0.95, 1.00)	**0.019***
Gabor	Standard deviation	0.95 (0.9, 0.99)	**0.026***
First order	Skewness	0.99 (0.98, 1.00)	0.0288
LoG	Kurtosis	0.68 (0.48, 0.96)	0.0301
LoG	Skewness	0.93 (0.86, 1.0)	0.036
Haralick	Energy	0.91 (0.83, 1.0)	0.04
Sobel	Kurtosis	0.87 (0.75, 1.0)	0.054
Sobel	Skewness	0.64 (0.39, 1.04)	0.073
Haralick	Correlation	0.9 (0.79, 1.03)	0.13
Haralick	Homogeneity	0.94 (0.87, 1.02)	0.139
First order	Kurtosis	1.02 (0.98, 1.06)	0.378
Gabor	Skewness	1.0 (0.96, 1.06)	0.862

*Significant after FDR correction.

Table 4 Multivariate analysis of the impact of mean LoG, ECOG, and LDH elevation on OS

	HR (95% CI)	*P*-value
Mean LoG	0.79 (0.6,1.03)	0.078
ECOG = 0	Reference	
ECOG = 1, 2, 3	1.84 (0.83, 4.09)	0.136
No LDH elevation	Reference	
LDH elevation	2.45 (1.16, 5.16)	**0.019**
ECOG * LDH elevation	0.41 (0.13, 1.3)	0.131

Table 5 Validation of model with an independent dataset

	P-value
Mean LoG[a,b]	**0.003**
ECOG = 0	Reference
ECOG = 1, 2, 3	**0.01**
No LDH elevation	Reference
LDH elevation	**0.03**

[a]Note the optimal cutoff for mean LoG was determined via the original data. The optimal cutoff value was 2.89, so we dichotomized mean LoG at this value in the validation data. [b]Univariate analysis was done due to the small sample size.

(P = 0.03). Utilizing the optimal cutoff for mean LoG of 2.89, higher mean LoG was significantly associated with OS (P = 0.003).

Discussion

This study analyzes higher-order MRI features in patients with melanoma brain metastases receiving ICIs. We found that several Haralick, Sobel, and Gabor radiomic features were associated with an improved OS; the results revealed potential associations between radiomic analysis and treatment response in this high-risk patient population. The association between the mean LoG feature and OS did not retain clinical significance on multivariate analysis incorporating LDH and performance status; however, the trend remained present. Additionally, mean LoG was confirmed to be significant in an independent dataset. Further analysis is required in larger, prospective cohorts of patients with melanoma brain metastases treated with more uniform therapies. This proof-of-concept study paves the way for further investigation, which may lead to a better understanding of the underlying biology evoked by radiomic features and the exact role they play in the management of patients.

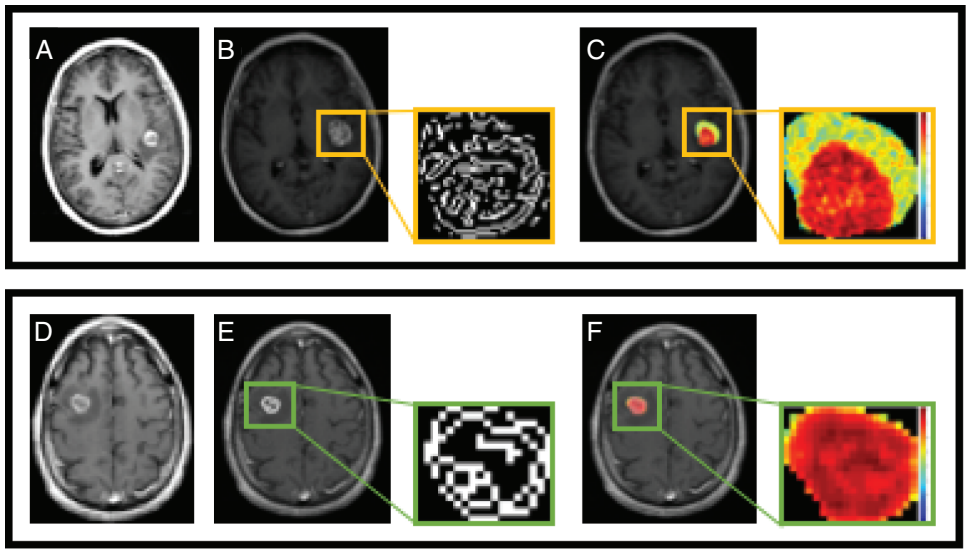

Fig. 2 MR images of a 56-year-old female patient with a left frontotemporal lobe melanoma brain metastasis that did not respond to ipilimumab and required unplanned radiation (upper panel), and a 75-year-old male patient with a right frontal lobe melanoma brain metastasis that had a complete response to ipilimumab (lower panel). Pretreatment post-contrast imaging is shown in (A) and (D) for each patient, respectively. Edge-filtered images for each metastatic lesion show that the LoG edges are more complex in the metastasis that progressed (B) compared with the metastasis that responded (E). Additionally, a representation of the extracted entropy feature shows there is higher entropy, highlighted by the increase in variation as well as disorder in the gray level distribution, in the progressing metastatic lesion (C) in comparison with the responding metastatic lesion (F).

Although higher-order features were associated with OS at univariate analysis, it is notable that they were not associated with PFS. In this study, any unplanned radiation, surgery, or change in targeted therapy due to an enlarging metastatic lesion was deemed progression, mimicking rules from prospective clinical trials. It is well described that some patients with melanoma brain metastases treated with checkpoint inhibitors can live long after progression.[9,10] We hypothesize that this apparent inconsistency may reflect the inherent difficulty radiologists and oncologists have in predicting patient outcomes from standard MRI results. Based on initial size increase, physicians may be utilizing stereotactic radiation prematurely in patients whose tumors possess higher-order texture features that would reflect a better long-term prognosis. This is particularly apropos in the patient who has possible pseudoprogression and other treatment changes; for example, the RANO-BM group has declared in these settings that "standard MRI alone is insufficient."[33] This study suggests that higher-order features, if validated in a larger, prospective cohort, could offer valuable insight to clinicians making difficult decisions on whether and when to add local radiation or change systemic therapy. Recently, combined nivolumab plus ipilimumab without SRS was shown to result in intracranial response rates in over 50% of carefully selected patients.[9,10] This underscores the importance of developing better imaging tools to distinguish whether a patient requires additional local or systemic therapy in the modern era of combination checkpoint inhibition.

While several studies have shown early promise for using radiomics in various malignancies,[16–30] no study has attempted to use radiomics to identify radiomic features predicting outcomes in brain metastases. This is likely due to the difficulty in accounting for the spatial and temporal relationships between different metastatic lesions that are present on brain imaging in each patient. We generated quantitative features that were then averaged over all brain metastases. While our approach suggests high prognostic capability, further work is necessary to account for the presence of intertumor genetic and transcriptomic variability. While there are no standard criteria for measuring heterogeneity in brain metastases with radiomics, we reexamined 45 patients who had multiple lesions and calculated the range of LoG within multiple lesions of each patient. Little variability was seen in patients with multiple lesions compared with between patients, consistent with genetic studies that report genetic homogeneity between patients with multiple metastatic lesions compared with the heterogeneous primary. Well-designed prospective studies that analyze brain metastases on a multidimensional level are needed so that the meaningful integration of imaging, histopathology, and genomic and epigenomic analysis can be done.

Our study has several limitations. This was a retrospective study and the indication for the initial MRI varied among patients, reflecting varying biology. Texture analysis was retrospectively obtained on the initial MRI; to limit bias, the experienced user who extracted features was blinded to the clinical history and outcomes of each patient. Because the initial inclusion period chosen for the retrospective cohort in this study spanned a number of years from 2010, only a minority of patients received PD1-based checkpoint inhibition, which is the current systemic therapy standard for patients with melanoma. Our smaller

validation cohort consisted of patients treated since 2016, and therefore these reflected the current standard practice of PD1 inhibition. MRI type and acquisition parameters were variable in order to maximize sample size. A more standardized approach for MRI acquisition should be considered in future studies for patients receiving frontline CTLA-4 and PD1-based therapy.

Several questions regarding the use of MRI radiomic features in brain metastases remain. Further studies should focus on the role texture features play in progression and pseudoprogression, specifically in the setting of immunotherapy. Understanding how texture signatures change over time or during the course of treatment would be helpful. It would be interesting to know if multi-parametric data that use several other sequences on the MRI might further strengthen the statistical significance; however, this introduces variability across institutions. Furthermore, radiomic signatures of brain metastases from other cancers such as breast and lung should be pursued as they are likely to be very different from melanoma brain metastases, which are often more hemorrhagic.

In summary, several Haralick, Gabor, and Sobel radiomic features were associated with an improved OS in patients with melanoma brain metastases receiving ICI. Additional prospective work is necessary to understand the ability of radiomic features to predict survival and to better understand the relationship between radiomic features and tumor heterogeneity.

Supplementary Material

Supplementary data are available at *Neuro-Oncology* online.

KeyWords

brain metastases | imaging biomarkers | immune checkpoint inhibitors | intratumoral heterogeneity | MRI radiomic features

Funding

This work was supported in part through the NIH/NCI Cancer Center Core Support Grant P30 CA008748, the Memorial Sloan Kettering (MSK) Brain Tumor Center, and the MSK Neuro-Oncology Research Translation in Humans Program.

Conflict of interest statement. Bianca D. Santomasso has consulted or participated in advisory boards for June Therapeutics/Celgene, Kite Pharma/Gilead, and Novartis. T. Jonathan Yang has ongoing research funded by AstraZeneca. Alexander N. Shoushtari has consulted or participated in advisory boards for Vaccinex, Castle Biosciences, Immunocore, and Bristol-Myers Squibb and has received research funding from Bristol-Myers Squibb, Immunocore, and Xcovery. Robert J. Young is a consultant for Agios, Puma, NordicNeuroLab, and Icon, and has received grant funding from Agios. No other authors have conflicts of interest.

Authorship statement:
A Bhatia, H Veeraraghavan, AN Shoushtari, and RJ Young designed the study.
A Bhatia, M Birger, H Veeraraghavan, H Um, AS McKenney, M Cugliari, A Caviasco, A Bialczak, R Malani, TJ Yang, B Santomasso, AN Shoushtari, and RJ Young collected the data.
A Bhatia, M Birger, H Veeraraghavan, H Um, F Tixier, AS McKenney, M Cugliari, A Caviasco, A Bialczak, R Malani, J Flynn, Z Zhang, TJ Yang, B Santomasso, AN Shoushtari, and RJ Young analyzed and interpreted the data.
A Bhatia, M Birger, H Veeraraghavan, H Um, F Tixier, AS McKenney, M Cugliari, A Caviasco, A Bialczak, R Malani, J Flynn, Z Zhang, TJ Yang, B Santomasso, AN Shoushtari, and RJ Young wrote the manuscript.
All authors approved the final manuscript.

References

1. Arvold ND, Lee EQ, Mehta MP, et al. Updates in the management of brain metastases. *Neuro Oncol.* 2016;18(8):1043–1065.
2. Davies MA, Liu P, McIntyre S, et al. Prognostic factors for survival in melanoma patients with brain metastases. *Cancer.* 2011;117(8):1687–1696.
3. Sampson JH, Carter JH Jr, Friedman AH, Seigler HF. Demographics, prognosis, and therapy in 702 patients with brain metastases from malignant melanoma. *J Neurosurg.* 1998;88(1):11–20.
4. Fife KM, Colman MH, Stevens GN, et al. Determinants of outcome in melanoma patients with cerebral metastases. *J Clin Oncol.* 2004;22(7):1293–1300.
5. Eigentler TK, Figl A, Krex D, et al; Dermatologic Cooperative Oncology Group and the National Interdisciplinary Working Group on Melanoma. Number of metastases, serum lactate dehydrogenase level, and type of treatment are prognostic factors in patients with brain metastases of malignant melanoma. *Cancer.* 2011;117(8):1697–1703.
6. Raizer JJ, Hwu WJ, Panageas KS, et al. Brain and leptomeningeal metastases from cutaneous melanoma: survival outcomes based on clinical features. *Neuro Oncol.* 2008;10(2):199–207.
7. Camidge DR, Lee EQ, Lin NU, et al. Clinical trial design for systemic agents in patients with brain metastases from solid tumours: a guideline by the response assessment in neuro-oncology brain metastases working group. *Lancet Oncol.* 2018;19(1):e20–e32.
8. Goldberg SB, Gettinger SN, Mahajan A, et al. Pembrolizumab for patients with melanoma or non-small-cell lung cancer and untreated brain metastases: early analysis of a non-randomised, open-label, phase 2 trial. *Lancet Oncol.* 2016;17(7):976–983.
9. Long GV, Atkinson V, Lo S, et al. Combination nivolumab and ipilimumab or nivolumab alone in melanoma brain metastases: a multicentre randomised phase 2 study. *Lancet Oncol.* 2018;19(5):672–681.
10. Tawbi HA, Forsyth PA, Algazi A, et al. Combined nivolumab and ipilimumab in melanoma metastatic to the brain. *N Engl J Med.* 2018;379(8):722–730.
11. Iorgulescu JB, Harary M, Zogg CK, et al. Improved risk-adjusted survival for melanoma brain metastases in the era of checkpoint blockade immunotherapies: results from a national cohort. *Cancer Immunol Res.* 2018;6(9):1039–1045.

12. Harbst K, Lauss M, Cirenajwis H, et al. Multiregion whole-exome sequencing uncovers the genetic evolution and mutational heterogeneity of early-stage metastatic melanoma. *Cancer Res.* 2016;76(16):4765–4774.
13. Gerlinger M, Rowan AJ, Horswell S, et al. Intratumor heterogeneity and branched evolution revealed by multiregion sequencing. *N Engl J Med.* 2012; 366(10):883–892.
14. Brastianos PK, Carter SL, Santagata S, et al. Genomic characterization of brain metastases reveals branched evolution and potential therapeutic targets. *Cancer Discov.* 2015;5(11):1164–1177.
15. Haralick RM. Statistical and structural approaches to texture. *P IEEE.* 1979; 67(5):786–804.
16. Haralick RM, Shanmugam K, Dinstein I. Textural features for image classification. *IEEE T Syst Man Cyb.* 1973; Smc3(6):610–621.
17. Hu L, Ning SL, Eschbacher J, et al. Radiogenomics to characterize regional genetic heterogeneity in glioblastoma. *Neuro Oncol.* 2016; 18:124.
18. Horvat N, Veeraraghavan H, Khan M, et al. MR imaging of rectal cancer: radiomics analysis to assess treatment response after neoadjuvant therapy. *Radiology.* 2018;287(3):833–843.
19. Zhou H, Vallières M, Bai HX, et al. MRI features predict survival and molecular markers in diffuse lower-grade gliomas. *Neuro Oncol.* 2017;19(6):862–870.
20. Liu J, Mao Y, Li Z, et al. Use of texture analysis based on contrast-enhanced MRI to predict treatment response to chemoradiotherapy in nasopharyngeal carcinoma. *J Magn Reson Imaging.* 2016;44(2):445.
21. De Cecco CN, Ganeshan B, Ciolina M, et al. Texture analysis as imaging biomarker of tumoral response to neoadjuvant chemoradiotherapy in rectal cancer patients studied with 3-T magnetic resonance. *Invest Radiol.* 2015;50(4):239–245.
22. Fox MJ, Gibbs P, Pickles MD. Minkowski functionals: an MRI texture analysis tool for determination of the aggressiveness of breast cancer. *J Magn Reson Imaging.* 2016;43(4):903–910.
23. Chen X, Wei X, Zhang Z, Yang R, Zhu Y, Jiang X. Differentiation of true-progression from pseudoprogression in glioblastoma treated with radiation therapy and concomitant temozolomide by GLCM texture analysis of conventional MRI. *Clin Imaging.* 2015;39(5):775–780.
24. Teruel JR, Heldahl MG, Goa PE, et al. Dynamic contrast-enhanced MRI texture analysis for pretreatment prediction of clinical and pathological response to neoadjuvant chemotherapy in patients with locally advanced breast cancer. *NMR Biomed.* 2014;27(8):887–896.
25. Yang D, Rao G, Martinez J, Veeraraghavan A, Rao A. Evaluation of tumor-derived MRI-texture features for discrimination of molecular subtypes and prediction of 12-month survival status in glioblastoma. *Med Phys.* 2015;42(11):6725–6735.
26. Hu LS, Ning S, Eschbacher JM, et al. Multi-parametric MRI and texture analysis to visualize spatial histologic heterogeneity and tumor extent in glioblastoma. *PLoS One.* 2015;10(11):e0141506.
27. Vallières M, Freeman CR, Skamene SR, El Naqa I. A radiomics model from joint FDG-PET and MRI texture features for the prediction of lung metastases in soft-tissue sarcomas of the extremities. *Phys Med Biol.* 2015;60(14):5471–5496.
28. Wibmer A, Hricak H, Gondo T, et al. Haralick texture analysis of prostate MRI: utility for differentiating non-cancerous prostate from prostate cancer and differentiating prostate cancers with different Gleason scores. *Eur Radiol.* 2015;25(10):2840–2850.
29. Veeraraghavan H, Dashevsky BZ, Onishi N, et al. Appearance constrained semi-automatic segmentation from DCE-MRI is reproducible and feasible for breast cancer radiomics: a feasibility study. *Sci Rep.* 2018;8(1):4838.
30. Lakhman Y, Veeraraghavan H, Chaim J, et al. Differentiation of uterine leiomyosarcoma from atypical leiomyoma: diagnostic accuracy of qualitative mr imaging features and feasibility of texture analysis. *Eur Radiol.* 2017;27(7):2903–2915.
31. Sutton EJ, Oh JH, Dashevsky BZ, et al. Breast cancer subtype intertumor heterogeneity: MRI-based features predict results of a genomic assay. *J Magn Reson Imaging.* 2015;42(5):1398–1406.
32. Okada H, Weller M, Huang R, et al. Immunotherapy response assessment in neuro-oncology: a report of the RANO working group. *Lancet Oncol.* 2015;16(15):e534–e542.
33. Lin NU, Lee EQ, Aoyama H, et al; Response Assessment in Neuro-Oncology (RANO) group. Response assessment criteria for brain metastases: proposal from the RANO group. *Lancet Oncol.* 2015;16(6):e270–e278.
34. Yushkevich PA, Piven J, Hazlett HC, et al. User-guided 3D active contour segmentation of anatomical structures: significantly improved efficiency and reliability. *Neuroimage.* 2006;31(3):1116–1128.
35. Apte AP, Iyer A, Crispin-Ortuzar M, et al. Technical note: extension of CERR for computational radiomics: a comprehensive MATLAB platform for reproducible radiomics research. *Med Phys.* 2018;45:3713–3720.
36. Fehr D, Veeraraghavan H, Wibmer A, et al. Automatic classification of prostate cancer Gleason scores from multiparametric magnetic resonance images. *Proc Natl Acad Sci U S A.* 2015;112(46):E6265–E6273.
37. Daugman JG. Uncertainty relation for resolution in space, spatial frequency, and orientation optimized by two-dimensional visual cortical filters. *J Opt Soc Am A.* 1985;2(7):1160–1169.
38. Tibshirani R. Regression shrinkage and selection via the Lasso. *J Roy Stat Soc B Met.* 1996; 58(1):267–288.
39. Tixier F, Um H, Bermudez D, et al. Preoperative MRI-radiomics features improve prediction of survival in glioblastoma patients over MGMT methylation status alone. *Oncotarget.* 2019;10(6):660–672.